Appl. Phys. A (2017)123:461
DOI 10.1007/s00339-017-1073-4

Applied Physics A
Materials Science & Processing

Effect of ordered B-site cations on the structure, elastic and thermodynamic properties of $KTa_{0.5}Nb_{0.5}O_3$ crystal

Wenlong Yang[1] · Junsheng Han[1] · Li Wang[1] · Yanqing Shen[2] · Linjun Li[3] · Yuqiang Yang[1] · Haidong Li[1] · Liangyu Chen[4]

Received: 28 December 2016 / Accepted: 30 May 2017

Abstract BO_6 oxygen octahedral was considered as the key part in ABO_3 perovskite structure, and the electro-optical, elastic and thermodynamic properties of potassium tantalate niobate ($KTa_{0.5}Nb_{0.5}O_3$, abbreviated as KTN) were closely depended on the B-site Ta/Nb ratio and ordering. The effect of $[100]_{NT}$, $[110]_{NT}$, and $[111]_{NT}$ B-site cations ordering (N means a pure Nb layer parallel to (h, k, l), T means a pure Ta layer parallel to (h, k, l)) on structure, elastic properties and Debye temperatures properties of KTN were investigated based on density functional theory (DFT). KTN with $[111]_{NT}$ B-site ordering presents an cubic phase structure with excellent stability from the view of lattice properties. The elastic properties include elastic stiffness coefficients C_{ij}, bulk modulus B, shear modulus G, Young's modulus E and Poisson' ratio v were calculated. The elastic stiffness coefficients C_{11} of KTN with B-site ordering have approached to maximum 485.506 GPa, indicating that KTN materials have better deformation ability along *x axis* compared with other perovskite materials. The calculated results of bulk modulus B and the shear modulus G show that KTN with $[100]_{NT}$ B-site ordering has stronger ability to resist fracture and plastic deformation. And the criteria B/G <1.75 suggests that KTN should be classified as a brittle material. The KTN with $[100]_{NT}$ B-site has excellent ductility properties compared with any other B-site arrangements. Debye temperatures of KTN with $[100]_{NT}$, $[110]_{NT}$, $[111]_{NT}$ are about 650 K, and KTN with $[100]_{NT}$ B-site has best thermodynamic stability.

1 Introduction

Elastic and thermodynamic properties are closely dependent on the atomic and electronic structure of material, which have attracted increasing attention and contributions to the investigation of actual electromechanical applications [1–3]. First-principles, a calculation method starts directly at the level of established laws of physics and does not make assumptions such as empirical model and fitting parameters, is widely used to explore the physical properties of materials from the aspect of electron and atom. Therefore, the theoretical calculation based on first-principles is an effective method to investigate functional materials, aiming to study the effects of local microstructure, and to expose the relationship between the inner structures and the electronic, mechanical, thermodynamic and optical properties of the materials. In recent years, the promising perovskite materials have been widely investigated [4, 5], and many achievements have been obtained on the ABO_3 perovskite materials with ordered structure through the theoretical methods, such as $PbTiO_3$ [6], $BaTiO_3$ [7, 8], $SrTiO_3$ [9] and $Sr_{1-x}Ca_xTiO_3$ [10].

✉ Wenlong Yang
yangwenlong1983@163.com

✉ Linjun Li
llj7897@163.com

[1] Department of Applied Science, Harbin University of Science and Technology, Harbin 150001, People's Republic of China

[2] Department of Physics, Harbin Institute of Technology, Harbin 150001, People's Republic of China

[3] Institute of Optoelectronic Technology, Heilongjiang Institute of Technology, Harbin 150050, China

[4] School of Material Science and Engineering, Jiangsu University of Science and Technology, Zhenjiang 212003, People's Republic of China

Published online: 02 June 2017

Potassium tantalate niobate $KTa_{1-x}Nb_xO_3$ (abbreviated as KTN) as a promising ABO_3 perovskite material is a compatible solid solution of $KNbO_3$ and $KTaO_3$. It has potential applications in electro-optic modulator, holography, sensor on account of the excellent electro-optic, ferroelectric, and piezoelectric performance [11–15]. The phase structures and the properties can be modulated by controlling the composition, and its Curie temperature of paraelectric–ferroelectric phase transition varies with the Ta/Nb ratio [16]. Wang et al. have calculated the electronic structure and optical properties of cubic and tetragonal $KTa_{0.5}Nb_{0.5}O_3$ based on the first-principles [17]. Moreover, the local B-site ordering of the Ta and Nb atoms has remarkable effects on the structural, optical and electrical properties as well [18, 19]. Xu et al. have presented the evidence for the existence of Ta–O–Nb link in KTN through the investigation of the local and long-range structures by powder diffraction and absorption fine structure (EXAFS) spectra, and found that the structure of the KTN could be controlled by the experimental condition and technology [20]. Shen et al. have reported the ordered B site cations have an important effect on the structural, electronic and optical performance of KTN [21, 22]. Considering elastic properties of KTN, Rytz et al. have reported that elastic compliance s_{11} measurements of KTN materials exhibited a concentration-dependent ferroelectric phase-transition temperature [23]. Then, the different elastic properties between paraelectric and ferroelectric phase of $KTa_{0.5}Nb_{0.5}O_3$ crystal have been calculated based on first principle, the results indicating that KTN with paraelectric phase is more incompressible and harder than that with ferroelectric phase [24].

To investigate the effects of local ordered structure on the mechanical, electronic, and thermodynamic of the materials, the elastic and thermodynamic properties of ordered B-site cations structures including $[100]_{NT}$, $[110]_{NT}$, $[111]_{NT}$ were calculated by first-principles density functional theory (DFT) method.

2 Computational and models

In this study, the first-principles calculation was performed based on the density functional theory (DFT) [25], and the exchange–correlation energy functional was implemented by the local density approximation (LDA) [26]. Under the LDA approximation, geometry optimizations were carried out by the Broyden–Fletcher–Goldfarb–Shannon (BFGS) algorithm and Vanderbilt-type ultrasoft pseudopotential (USP) [27]. In geometry optimization and elastic computing, the total energy variation was 5×10^{-6} eV/atom, maximum force for per atom was 0.01 eV/Å, the maximum stress was 0.02 GPa, and the maximum displacement of atom was 5×10^{-4} eV/Å. The energy cut-off of the plane wave basis was set as 380 eV, the valence electrons considered were K (3s, 3p, and 4s), Ta (5d and 6s), Nb (4d and 5s) and the O (2s and 2p). The sampling of the Brillouin zone was of $3 \times 3 \times 3$ *k*-points with a Monkhorst–Pack grid [21, 28], and *k*-points separation was always less than 0.04/Å. The results were tested for convergence with respect to the number of *k*-point and the cut-off energy.

All of the possible arrangements of B sites Ta/Nb atomics within 40-atom cells (the $2 \times 2 \times 2$ ordered KTN supercells) were designed and calculated. The structures of KTN crystal with ordered B-site cations are showed in Fig. 1, where (a) $[100]_{NT}$, (b) $[110]_{NT}$, (c) $[111]_{NT}$ represent three different arrangement, respectively. Here, the subscript N means a pure Nb layer parallel to (*h*, *k*, *l*); and the subscript T means a pure Ta layer parallel to (*h*, *k*, *l*).

3 Results and discussions

3.1 Lattice properties

The value of calculated lattice parameters and volumes of $[100]_{NT}$, $[110]_{NT}$, $[111]_{NT}$ from the geometry optimization are listed in Table 1. The calculated lattice parameters are in excellent agreement with the experimental values for solid solution KTN with *a* 4.00289, 4.00251 and 3.99279 Å corresponding to three different Ta/Nb ratios are 0.65/0.35, 0.55/0.45 and 0.35/0.65, respectively [29]. Different B-site ordered KTN crystals present tetragonal ferroelectric and cubic phase through geometry optimization. The space group of KTN with $[100]_{NT}$ and $[110]_{NT}$ belong to P4/mmm, and the space group of KTN with $[111]_{NT}$ belongs to Fm3m. In addition, the lattice parameters of KTN have inconspicuous variation for Ta, Nb atomic location in oxygen octahedrons structure, because of these approximate particle radiuses.

3.2 Elastic properties and mechanical stability

Elastic stiffness constants are the key characteristic parameters for mechanical and dynamical behaviors, which can also provide significant information with respect to the elastic response to an external applied stress and are determined by Hooke's law. The investigation of elastic constants can be realized by electronic structure based on the density function theory. To calculate elastic constants of different B-site ordered KTN, we employed the stress–strain method, which can be depicted as follows [30]:

$$(\sigma_1, \sigma_2, \sigma_3, \sigma_4, \sigma_5, \sigma_6) = C(\varepsilon_1, \varepsilon_2, \varepsilon_3, \varepsilon_4, \varepsilon_5, \varepsilon_6)^T, \quad (1)$$

where *C* is the elastic stiffness matrix.

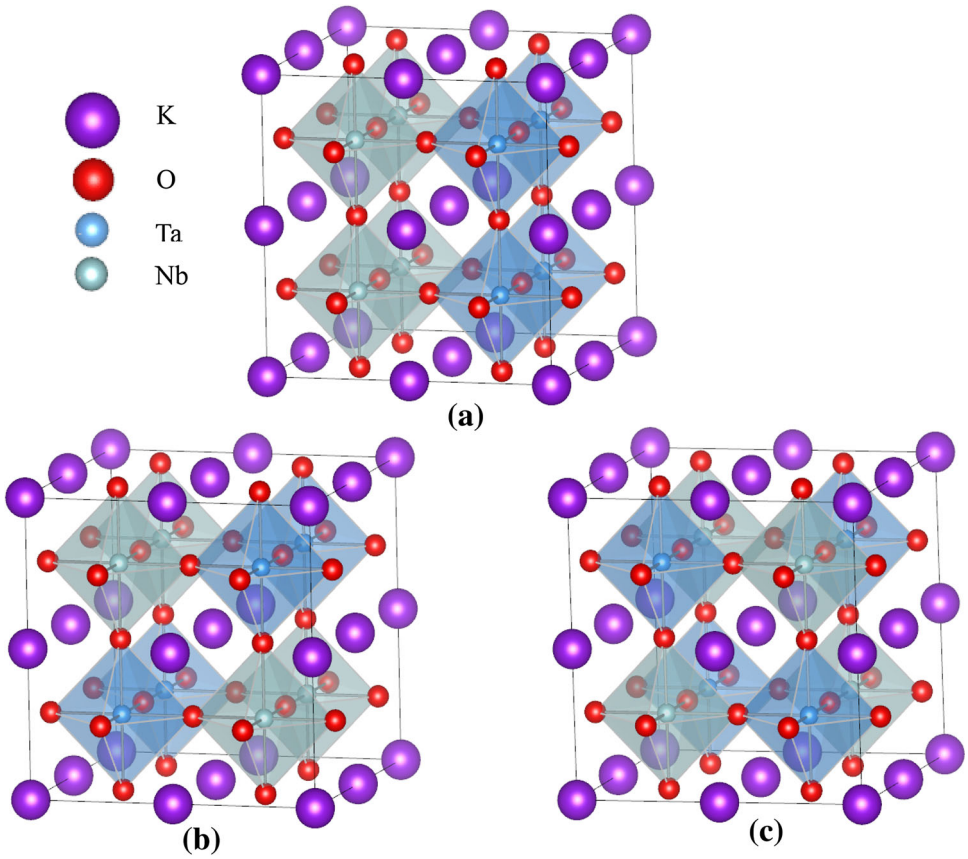

Fig. 1 Supercell of KTN with **a** $[100]_{NT}$, **b** $[110]_{NT}$, **c** $[111]_{NT}$ B-site ordering

Table 1 The calculated results about structure parameters and formation energies of KTN with (a) $[100]_{NT}$ (b) $[110]_{NT}$ (c)$[111]_{NT}$ B-site ordering

B-site ordering	a (Å)	b (Å)	c (Å)	V (Å^3)
$[100]_{NT}$	7.996	7.996	7.974	509.720
$[110]_{NT}$	7.978	7.978	7.997	509.000
$[111]_{NT}$	7.981	7.981	7.981	508.360

There are only three independent elastic stiffness coefficients (C_{11}, C_{12} and C_{44}) for the cubic crystal, each of which represents three equal elastic constants ($C_{11} = C_{22} = C_{33}$, $C_{12} = C_{23} = C_{31}$ and $C_{44} = C_{55} = C_{66}$). The requirement of the mechanical stability in a cubic crystal possesses the following restrictions on the elastic constants [31];

$$C_{11} > 0, C_{44} > 0, C_{11} > |C_{12}|, C_{11} + 2C_{12} > 0, \text{ and } C_{12} < B < C_{11}, \quad (2)$$

where B is bulk modulus of the material.

For the Tetragonal phase crystal, there are six independent elastic stiffness coefficients (C_{11}, C_{12}, C_{13}, C_{33}, C_{44} and C_{66}), with $C_{11} = C_{22}$, $C_{13} = C_{23}$, $C_{44} = C_{55}$. The mechanical stability criterion (i.e., the well-known Born's criteria) can be written as following [32]:

$$C_{11} > 0, C_{33} > 0, C_{44} > 0, C_{66} > 0, C_{11} - C_{12} > 0, \quad C_{11} + C_{33} - 2C_{13} > 0,$$
$$2(C_{11} + C_{12}) + C_{33} + 4C_{13} > 0, \text{ and } \frac{1}{3}(C_{12} + 2C_{13}) < B < \frac{1}{3}(C_{11} + 2C_{33}). \quad (3)$$

The calculated values of the elastic stiffness constants of KTN with $[100]_{NT}$, $[110]_{NT}$, and $[111]_{NT}$ arrangements are listed in Table 2. The $[100]_{NT}$ B-site ordered KTN with the elastic constants $C_{11} = 485.506$, $C_{33} = 496.138$, $C_{44} = 86.992$, $C_{66} = 86.458$, $C_{12} = 72.066$, $C_{13} = 72.061$ and the bulk modulus $B = 212.066$ are in accord with all the inequality in criterion (3). The $[110]_{NT}$ B-site ordered KTN with the elastic constants $C_{11} = 481.986$, $C_{33} = 496.156$, $C_{44} = 86.648$, $C_{66} = 86.869$, $C_{12} = 76.158$, $C_{13} = 71.697$ and bulk modulus $B = 211.040$ are also in accord with all the inequality in criterion (3). These indicate that KTN with $[100]_{NT}$ and $[110]_{NT}$ arrangements are mechanically stable. The $[111]_{NT}$ B-site ordered KTN with the elastic constants $C_{11} = 478.927$, $C_{44} = 86.802$, $C_{12} = 75.807$ and bulk modulus $B = 210.181$ are in accord with all the inequality in criterion (2), which means that KTN with

Table 2 The elastic stiffness constants C_{ij} of B-site $[100]_{NT}$, $[110]_{NT}$ and $[111]_{NT}$ ordered KTN

C_{ij} (GPa)	$[100]_{NT}$	$[110]_{NT}$	$[111]_{NT}$	Calc.	$BaTiO_3$	$CaTiO_3$	$PbTiO_3$	$SrTiO_3$
C_{11}	485.506	481.986	478.927	489.0866	317.96	277.3	253.9	226.5
C_{33}	496.138	496.156	–	472.4396	318.43	358.1	79.8	316.0
C_{44}	86.992	86.648	86.802	87.9732	126.74	109.2	73.3	103.1
C_{66}	86.458	86.869	–	84.1298	126.72	120.5	100.9	118.6
C_{12}	72.066	76.158	75.807	65.1750	111.07	92.4	103.8	−0.8
C_{13}	72.061	71.697	–	64.7585	111.11	113.1	79.0	175.5

$[111]_{NT}$ arrangement is mechanically stable. Therefore, it is clear that the KTN with different arrangements are mechanically stable. And the results are in agreement with the previous calculations mainly about elastic properties of different phase structure [24]. The $[100]_{NT}$ B-site ordered KTN with the elastic constants $C_{11} = 485.506$ and $C_{33} = 496.138$, which are much larger than these parameters of $BaTiO_3$, $CaTiO_3$, $PbTiO_3$, and $SrTiO_3$ referred in Table 2 [33], which indicates that the KTN crystals possess excellent deformation ability along x and z orientation. Moreover, the different B-site ordered KTN presents various elastic stiffness constants, the C_{11} and C_{44} of $[100]_{NT}$ oriented arrangement are larger than that of KTN with the other B-site ordering arrangement, which indicates that$[100]_{NT}$ oriented arrangement has better deformation ability along *x axis*.

The elastic properties are determined by the bulk modulus B, shear modulus G, Young' s modulus E, and Poisson' s ratio v, which obviously play an important role in the strength of the materials as well. The calculated results of the bulk modulus B and shear modulus G are listed in Table 3. The bulk modulus B represents the resistance to fracture, whereas the shear modulus G represents the resistance to plastic deformation. We calculated KTN crystal's bulk modulus and shear modulus in the Voigt approximation (B_V, G_V) [34] and in the Reuss approximation (B_R, G_R) [35], then the Voigt–Reuss–Hill approximation (B, G) was utilized as follows:

$$B = \frac{B_V + B_R}{2}, \tag{4}$$

and

$$G = \frac{G_V + G_R}{2}. \tag{5}$$

For cubic symmetry, the Voigt and Reuss approximation for bulk and the shear modulus can be expressed by elastic stiffness constants as followS [36]:

$$B_V = B_R = \frac{(C_{11} + 2C_{12})}{3}, \tag{6}$$

$$G_V = \frac{(C_{11} - C_{12} + 3C_{44})}{5}, \tag{7}$$

$$G_R = \frac{5(C_{11} - C_{12})C_{44}}{[4C_{44} + 3(C_{11} - C_{12})]}. \tag{8}$$

For the tetragonal symmetry, the B_V, B_R, G_V, and G_R parameters can be also given by a combination of elastic stiffness coefficients [37].

$$B_V = \frac{1}{9}[2(C_{11} + C_{12}) + C_{33} + 4C_{13}], \tag{9}$$

$$G_V = \frac{1}{30}(M + 3C_{11} - 3C_{12} + 12C_{44} + 6C_{66}), \tag{10}$$

$$B_R = \frac{C^2}{M}, \tag{11}$$

$$G_R = 15\left\{\left(\frac{18B_V}{C^2}\right) + \left[\frac{6}{(C_{11} - C_{12})}\right] + \left(\frac{6}{C_{44}}\right) + \left(\frac{3}{C_{66}}\right)\right\}^{-1}, \tag{12}$$

where the M, C^2 parameters can be written as

$$M = C_{11} + C_{12} + 2C_{33} - 4C_{13}, \tag{13}$$

$$C^2 = (C_{11} + C_{12})C_{33} - 2C_{13}^2. \tag{14}$$

The Young's modulus (E) is the ratio of stress to strain on the loading plane along the loading direction, and the Poisson's ratio (v) is defined as the ratio of lateral strain and axial strain, and provides more information about bonding forces. The Young's modulus E and Poisson' s

Table 3 The bulk modulus B (GPa), shear modulus G (GPa), Young's modulus E (GPa) and Poisson's ratio v of B-site $[100]_{NT}$, $[110]_{NT}$ and $[111]_{NT}$ ordered KTN

Elastic parameters	$[100]_{NT}$	$[110]_{NT}$	$[111]_{NT}$
B_V (GPa)	212.074	211.048	210.181
B_R (GPa)	212.057	211.032	210.181
G_V (GPa)	136.140	134.743	132.698
G_R (GPa)	113.289	112.944	112.399
B (GPa)	212.066	211.040	210.181
G (GPa)	124.715	123.844	122.549
E (GPa)	312.821	310.689	307.820
B/G	1.700	1.704	1.715
v	0.258	0.255	0.256

ratio v are often used for evaluating the hardness of materials and can be computed by the following equations [37], respectively

$$E = \frac{9BG}{3B + G}, \tag{15}$$

$$v = \frac{3B - 2G}{2(3B + G)}. \tag{16}$$

The value B/G is proposed by Pugh and related to the brittle and ductile behavior of materials [38]. If the value $B/G > 1.75$, the material will behave in a ductile manner or else the material manifests brittleness. The calculated results of bulk modulus B and shear modulus G, the B/G, Young' s modulus E, and Poisson's ratio v are given in Table 3. According to these values, we find the magnitude of B, G, E has the same trend: $[100]_{NT} > [110]_{NT} > [111]_{NT}$. And the results show that $[100]_{NT}$ B-site ordering has stronger ability to resist fracture and plastic deformation. The obtained B/G ratios are all lower than 1.75 for these models, which demonstrates KTN should be classified as a brittle material. The value of Poisson's ratio v is associated with volume change during uniaxial deformation, and provides more information about the characters of the bounding forces than any other elastic constants. The calculated Poisson' ratios (v) of three models are larger than the value 0.25, which indicates the inter-atomic forces of KTN are central.

The elastic anisotropy of KTN with different B-site arrangements is significant for mechanical properties, which can be analyzed by elastic anisotropy index A^U for all crystal with different phases [39]. The anisotropy fraction ratio was presented by Chung and Buessem [40], which was shown as following:

$$A^U = 5\frac{G_V}{G_R} + \frac{B_V}{B_R} - 6, \tag{17}$$

$$A_B = \frac{B_V - B_R}{B_V + B_R}, \tag{18}$$

$$A_G = \frac{G_V - G_R}{G_V + G_R}, \tag{19}$$

where A_B, A_G represent the anisotropic degrees of bulk and shear modulus, respectively. For the isotropic materials, $A^U = 0$, $A_B = 0$, $A_G = 0$. The material possesses stronger anisotropy when the value A^U is larger. Moreover, the material presents strong anisotropic when A_B, A_G are 1. From the calculated values in Table 4, The KTN with B-site $[100]_{NT}$ ordering has excellent elastic anisotropy on account of large elastic anisotropy index. From the view of anisotropy fraction ratio, the anisotropy fraction ratio of bulk modulus is obviously lower than anisotropy fraction ratio of shear modulus. It is easy to point that the elastic anisotropy of KTN with B-site $[100]_{NT}$ ordering is best still compared with that of another KTN with different B-site orderings. Therefore, the elastic properties of KTN materials show anisotropic, and elastic anisotropy of KTN with B-site $[100]_{NT}$ ordering are obviously strong.

Table 4 The elastic anisotropy index A^U and anisotropy fraction ratio A_B and A_G of B-site [100]NT, [110]NT and [111]NT ordered KTN

B-site ordering	A^U	A_B	A_G
$[100]_{NT}$	1.009	4.095×10^{-5}	0.092
$[110]_{NT}$	0.965	3.897×10^{-5}	0.088
$[111]_{NT}$	0.903	2.379×10^{-8}	0.083

3.3 Debye temperatures

Debye temperature (θ_D) is a fundamental parameter in solid-state physics, which closely related to lattice vibration and elastic properties. The calculated Debye temperature of KTN can be estimated by elastic constants and the averaged sound velocity (v_m), the longitudinal sound velocity (v_l) and transverse sound velocity (v_t) as following [41]

$$\theta_D = \frac{h}{k_B}\left[\frac{3n}{4\pi}\left(\frac{N_A\rho}{M}\right)\right]^{\frac{1}{3}} v_m, \tag{20}$$

$$v_m = \left[\frac{1}{3}\left(\frac{2}{v_t^3} + \frac{1}{v_l^3}\right)\right]^{-\frac{1}{3}}, \tag{21}$$

$$v_l = \left[\left(B + \frac{4}{3}G\right)\frac{1}{\rho}\right]^{\frac{1}{2}}, \tag{22}$$

$$v_t = \left(\frac{G}{\rho}\right)^{\frac{1}{2}}, \tag{23}$$

where h and k_B are Planck's and Boltzmann's constants, respectively. N_A is Avogadro' s number, ρ is the density, M is the molecular weight, and n is the number of atoms in a formula unit.

The calculated values of v_m, v_l, v_t and θ_D of KTN with $[100]_{NT}$, $[110]_{NT}$, and $[111]_{NT}$ B-site orderings are given in Figs. 2 and 3, respectively. The calculated values of averaged sound velocity (v_m), the longitudinal sound velocity (v_l) and transverse sound velocity (v_t) in KTN with $[100]_{NT}$ B-site ordering are slightly higher than that with $[110]_{NT}$ and $[111]_{NT}$ B-site orderings. In addition, the calculated Debye temperatures θ_D of KTN with $[100]_{NT}$ B-site ordering is highest of all, indicating that atomic binding forces in KTN structure with $[100]_{NT}$ B-site ordering is strong, which demonstrates large hardness and high melting point. Therefore, B-site ordering has significant influences on thermodynamic properties.

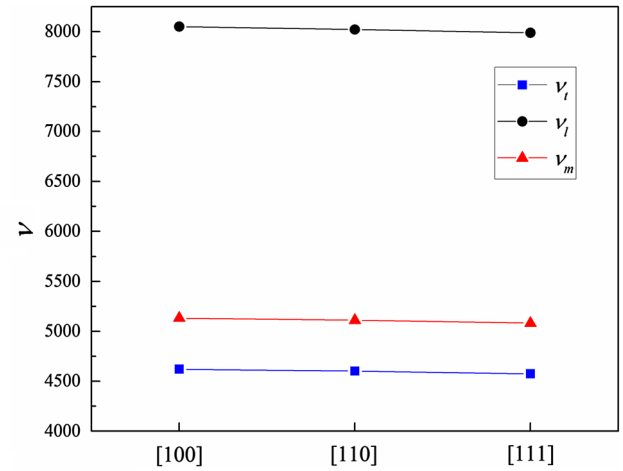

Fig. 2 The averaged sound velocity (v_m), the longitudinal sound velocity (v_l), transverse sound velocity (v_t) of B-site $[100]_{NT}$, $[110]_{NT}$ and $[111]_{NT}$ ordered KTN

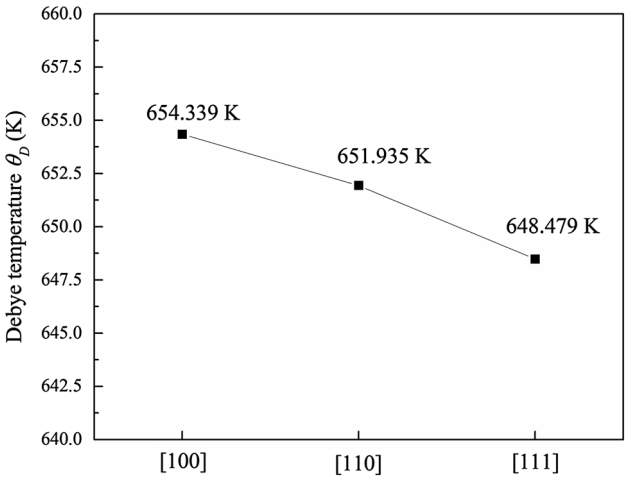

Fig. 3 Debye temperature θ_D of B-site $[100]_{NT}$, $[110]_{NT}$ and $[111]_{NT}$ ordered KTN

4 Conclusions

The atomic structure, elastic properties and Debye temperatures properties of KTN with $[100]_{NT}$, $[110]_{NT}$, and $[111]_{NT}$ B-site ordering were investigated using first-principles based on DFT within LDA-PZ method. KTN with $[111]_{NT}$ B-site ordering possesses excellent stability and presents cubic phase structure, and KTN with $[110]_{NT}$, and $[111]_{NT}$ ordered B-site show tetragonal phase. The elastic coefficients of KTN cubic phase structure, the C_{11} of $[100]_{NT}$ oriented arrangement is 485.506 GPa, which obviously higher than other materials, and the KTN with $[100]_{NT}$ oriented arrangement has better deformation ability along *x axis*. The bulk modulus *B* and the shear modulus *G* of $[100]_{NT}$ B-site ordering are 212.066 and 124.715 GPa, respectively, indicating KTN with $[100]_{NT}$ B-site ordering has stronger ability to resist fracture and plastic deformation. The obtained *B/G* ratio of $[100]_{NT}$, $[110]_{NT}$, and $[111]_{NT}$ ordered B-site arrangements are 1.700, 1.704 and 1.715, respectively, which demonstrates that KTN should be classified as a brittle material. KTN with $[100]_{NT}$ B-site ordering possesses excellent hardness properties with Young' s modulus *E* 312.82 GPa. The calculated Poisson' ratio (v) of KTN with B-site ordering provides more information about the characteristics of the bounding forces; the value (v) is larger than 0.25 indicates the interatomic forces of KTN are central. The elastic anisotropy index A^U and anisotropy fraction ratio A_B and A_G both demonstrate that the elastic properties of KTN materials are anisotropic, and the elastic anisotropy of KTN with B-site $[100]_{NT}$ ordering are obviously strong. Therefore, the KTN with B-site $[100]_{NT}$ ordering has excellent elastic properties. The averaged sound velocity (v_m), the longitudinal sound velocity (v_l), transverse sound velocity (v_t) and the Debye temperature (θ_D) were obtained by means of calculation. For all calculated values, the Debye temperatures of three modes are about 650 K, the trend is $[100]_{NT}$>$[110]_{NT}$>$[111]_{NT}$, so $[100]_{NT}$ has best thermodynamic stability.

Acknowledgements This work was supported by the Natural Science Foundation of China (No. 11444004), and the Natural Science Foundation of Heilongjiang Province (No. QC2015062).

References

1. Z. Tylczynski, P. Busz, Mater. Chem. Phys. **183**, 254 (2016)
2. C.J. Wang, J.B. Gu, W.X. Zhang, B. Sun, D.D. Liu, G.Q. Liu, Comput. Mater. Sci. **124**, 375 (2016)
3. W.H. Chen, H.C. Cheng, C.F. Yu, J. Alloy. Compd. **689**, 857 (2016)
4. H. Tian, C.P. Hu, Q.Z. Chen, Z.X. Zhou, Mater. Lett. **68**, 14 (2012)
5. H. Tian, Z.X. Zhou, D.W. Gong, H.F. Wang, Y.Y. Jiang, C.F. Hou, Opt. Commum. **281**, 1720 (2008)
6. W.Q. Huang, H. Yang, G.W. Lu, Y.N. Gao, Phys. B **411**, 56 (2013)
7. J.J. Wang, F.Y. Meng, X.Q. Ma, M.X. Xu, L.Q. Chen, J. Appl. Phys. **108**, 034107 (2010)
8. A. Mahmoud, A. Erba, E. El-Kelany Kh, M. Rérat, R. Orlando, Phys. Rev. B **89**, 045103 (2014)
9. C.E. Ekuma, M. Jarrell, J. Moreno, D. Bagayoko, AIP Adv. **2**, 012189 (2012)
10. C.Y. Yang, R. Zhang, Chin. Phys. B **23**, 026301 (2014)
11. S. Riehemann, D. Sabbert, S. Loheide, F. Matthes, G. von Bally, E. Kratzig, Opt. Mater. **4**, 437 (1995)
12. H. Tian, Z. Zhou, D. Gong, H. Wang, D. Liu, Y. Jiang, Appl. Phys. B **91**, 75 (2008)
13. H. Tian, B. Yao, P. Tan, Z.X. Zhou, G. Shi, D.W. Gong, R. Zhang, Appl. Phys. Lett. **106**, 102903 (2015)
14. M. Shinagawa, J. Kobayashi, S. Yagi, Y. Sakai, Sensor Actuators A Phys. **192**, 42 (2013)
15. X.J. Zheng, H.Y. Zhao, X.P. Wang, B. Liu, J.D. Yu, X.L. Zhao, Ceram. Int. **41**, S197 (2015)

16. K.Y. Zheng, D.M. Zhang, Z.C. Zhong, F.X. Yang, X.Y. Han, Appl. Surf. Sci. **256**, 1317 (2009)
17. Y.X. Wang, W.L. Zhong, C.L. Wang, P.L. Zhang, Opt. Commun. **201**, 79 (2002)
18. W.L. Yang, Z.X. Zhou, B. Yang, Y.Y. Jiang, H. Tian, D.W. Gong, H.G. Sun, W. Chen, Appl. Surf. Sci. **257**, 7221 (2011)
19. H.G. Wu, S.M. Wang, Z.X. Xu, J. Fu, Mater. Lett. **57**, 2742 (2003)
20. J. Xu, A.P. Wilkinson, S. Pattanaik, Chem. Mater. **13**, 1185 (2001)
21. Y.Q. Shen, Z.X. Zhou, Comput. Mater. Sci. **42**, 434 (2008)
22. Y.Q. Shen, Z.X. Zhou, Comput. Mater. Sci. **41**, 542 (2008)
23. D. Rytz, A. Châtelain, U.T. Höchli, Phys. Rev. B **27**, 6830 (1983)
24. Y. Wang, Y.Q. Shen, Z.X. Zhou, Phys. B **406**, 850 (2011)
25. W. Kohn, L.J. Sham, Phys. Rev. **140**, A1133 (1965)
26. D.M. Ceperley, B.J. Alder, Phys. Rev. Lett. **45**, 566 (1980)
27. D. Vanderbilt, Phys. Rev. B **41**, 7892 (1990)
28. H.J. Monkhorst, J.D. Pack, Phys. Rev. B **13**, 5188 (1976)
29. X. Wang, J. Wang, Y. Yu, H. Zhang, R.I. Boughton, J. Cryst. Growth **293**, 398 (2006)
30. O.H. Nielsen, R.M. Martin, Phys. Rev. B **32**, 3792 (1985)
31. J.P. Long, Phys. B **407**, 4831 (2012)
32. S. Piskunov, E. Heifets, R.I. Eglitis, G. Borstel, Comput. Mater. Sci. **29**, 165 (2004)
33. J. Long, L. Yang, X. Wei, J. Alloy. Compd. **549**, 336 (2013)
34. W. Voigt, in *Lehrbuch der Kristallphysik*, (L. Berlin, B.G. Teubner, Germany, 1928), p. 960
35. A. Reuss, Z. Angew, Math. Mech. **9**, 49 (1929)
36. Z.J. Wu, E.J. Zhao, H.P. Xiang, X.F. Hao, X.J. Liu, J. Meng, Phys. Rev. B **76**, 054115 (2007)
37. E. Schreiber, O.L. Anderson, N. Soga, Elastic Constants and Their Measurement (McGraw-Hill, New York, 1973)
38. S.F. Pugh, Philos. Mag. **45**, 823 (1954)
39. S.I. Ranganathan, M. Ostoja-Starzewski, Phys. Rev. Lett. **101**, 055504 (2008)
40. D.H. Chung, W.R. Buessem, J. Appl. Phys. **38**, 2010 (1967)
41. O.L. Anderson, J. Phys. Chem. Solids **24**, 909 (1963)